JOURNAL OF MATERIALS SCIENCE 31 (1996) 1199–1204

Equivalent network characterization for dielectric materials

H. S. B. ELAYYAN, S. N. AL-REFAIE*
Faculty of Engineering, Mu'tah University, Karak, Jordan

This paper presents a novel approach to the characterization of dielectrics exhibiting dispersion with frequency and the derivation of their equivalent circuits. The approach is based on the utilization of generalized relaxation time distribution (GRTD) facilitated by the analysis of dispersion in the dielectric constant complex plane. New parametric characterizations are introduced leading to a direct derivation of a distributed resistance–capacitance (R–C) network. The validity of this new methodology is examined by comparing reported measurements of a.c. resistivity and permittivity of zinc oxide (ZnO) varistors with those obtained from distributed parameter predictions. A discrete form of the equivalent network is also derived consisting of 16 R–C branches. The results of the distributed parameters and discrete equivalent network will be shown to agree satisfactorily with measurements over the frequency range of 30 Hz to 10 MHz. Remarkable agreement was also obtained between measured dispersion and network predictions for a perfluoropolyether microemulsion polymer over the frequency range of about 100 kHz up to 100 MHz using 18 R–C branches.

1. Introduction

The performance of electrical and electronic systems, subjected to electric fields of variable magnitude and frequency, is partly determined by the behaviour of dielectric materials. In such systems, characterization methods that allow the development of equivalent circuit representation are required for several engineerin ⊱ g objectives. A quantitative comparison between the electrical properties of different types of dielectric materials can be drawn in terms of equivalent circuit parameters. Most importantly, those circuits can effectively be used to investigate the anomalous behaviour exhibited by the majority of dielectric materials employed in engineering applications.

Well developed dielectric analysis is more or less confined to dielectrics characterized by single relaxation time. However, the majority of dielectrics, linear and nonlinear, cannot be accounted for using the simplified, single-relaxation Debye treatments. Their dispersion characteristics with frequency indicate many relaxation times. The lack of a generalized formulation for dielectrics has made it difficult to derive equivalent circuits which accurately simulate their behaviour over the full frequency range. Previous attempts to develop equivalent circuits fall short of covering practical frequency ranges. The bases adopted in those circuit developments relied mainly on data fitting thus reflecting a limited range of measured data [1–5].

The characteristics of many relaxation times is accounted for by the recently developed multiple-arc analysis whereby circular arcs are described in the dielectric constant complex plane [6, 7]. The analysis has facilitated the development of a generalized distribution for relaxation time (GRTD). Introducing a new parametric characterization for dispersion has enabled the derivation of an equivalent circuit based on a distributed network [8–10]. In this paper, a discrete form is derived for the equivalent circuit. To examine the validity of this new methodology, reported measurements on zinc oxide varistors at low fields and perfluoropolyether microemulsion polymer are compared with calculated results from both the distributed and discrete networks.

2. Dielectric characterization and equivalent circuit

For a dielectric material characterized by a single relaxation time, m a simple series resistance–capacitance (R–C) in parallel with a high-frequency capacitance C_∞, corresponds adequately to the variation of the equivalent parallel resistance and capacitance with frequency (see Fig. 1) and thus accounts for the dispersion of dielectric constant with frequency [11]. Accordingly, for a dielectric material with multiple relaxation times, the equivalent circuit consists of many R–C branches connected in parallel (see Fig. 2) [11]. With σ and ε representing the resistive and capacitive elements, respectively, a branch conductivity is given by

$$\sigma_k(\omega) = \frac{\omega^2 \tau_k \varepsilon_k}{(1 + \omega^2 \tau_k^2)} \quad (1)$$

Present address: Faculty of Applied Engineering, Yarmouk University, Irbid, Jordan.

0022–2461

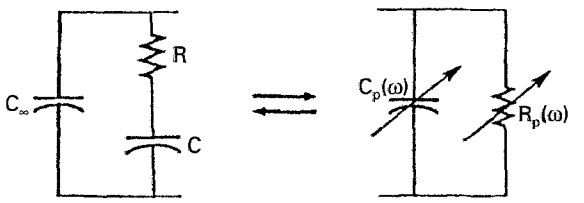

Figure 1 The series R–C circuit and its parallel equivalent representing the semicircular dispersion relation.

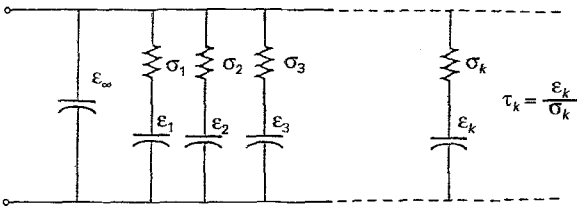

Figure 2 Equivalent circuit representing the circular arc dispersion relation.

and consequently, the total a.c. conductivity becomes

$$\sigma_t(\omega) = \sum_{k=1}^{L} \frac{\omega^2 \tau_k \varepsilon_k}{(1 + \omega^2 \tau_k^2)} \quad (2)$$

where k designates a branch of τ_k time constant with $\tau_k = \varepsilon_k/\sigma_k$. L is the number of branches representing the dispersion over the frequency range of interest.

From the extended multiple-arc analysis of complex dielectric constant, the GRTD is given by [7],

$$f(u) = C \sum_{n=1}^{m} \frac{(\varepsilon_{sn} - \varepsilon_{\infty n}) \sin(\alpha_n \pi)}{\cosh[(1 - \alpha_n)(u + \beta_n)] - \cos(\alpha_n \pi)} \quad (3)$$

where

$$C = \left[2\pi \sum_{n=1}^{m} (\varepsilon_{sn} - \varepsilon_{\infty n}) \right]^{-1}, \beta_n = \ln(\tau_{oII}/\tau_{on}),$$

and $u = \ln(\tau/\tau_{oII})$. n designates an arc which is specified by the static dielectric constant ε_{sn}, the high frequency dielectric constant $\varepsilon_{\infty n}$ and the parameter of relaxation spread α_n. α_n takes a value between 0 and 1; $\alpha_n = 0$ corresponds to a semicircular relation. τ_{on} is a characteristic relaxation time of the nth arc, while τ_{oII} is the low frequency reference arc. m designates the number of arcs determined over the frequency range used [7].

By expressing the complex dielectric constant, $\varepsilon^* = \varepsilon' - j\varepsilon''$, in terms of the relaxation-time domain, the imaginary component is expressed as [12],

$$\varepsilon''(\omega) = \sum_{n=1}^{m} (\varepsilon_{sn} - \varepsilon_{\infty n}) \int_{-\infty}^{\infty} \frac{\omega \tau f(u)}{(1 + \omega^2 \tau^2)} \partial u \quad (4)$$

Using the relationship $\sigma = \varepsilon_o \varepsilon'' \omega$, and with ω being independent of the variable u, the total a.c. conductivity of the dielectric becomes

$$\sigma_t(\omega) = \varepsilon_o \sum_{n=1}^{m} (\varepsilon_{sn} - \varepsilon_{\infty n}) \int_{-\infty}^{\infty} f(u) \frac{\omega^2 \tau}{(1 + \omega^2 \tau^2)} \partial u \quad (5)$$

The continuous distribution of relaxation times implies a continuous distributed network. In order to facilitate derivation of the network, the following distribution parameters are defined [8].

$$\bar{\varepsilon}(u) = \frac{\partial \varepsilon(u)}{\partial u}$$

and

$$\bar{\sigma}(u) = \frac{\partial \sigma(u)}{\partial u}$$

with

$$\tau = \frac{\varepsilon_o \bar{\varepsilon}(u)}{\bar{\sigma} u}$$

Subsequently, Equation 2 takes the following integral form, as $L \to \infty$ and $\varepsilon_k \to \partial\varepsilon$ for a continuous system,

$$\sigma_t(\omega) = \int_{-\infty}^{\infty} \varepsilon_o \bar{\varepsilon}(u) \frac{\omega^2 \tau}{(1 + \omega^2 \tau^2)} \partial u \quad (6)$$

The integral limits corresponds to $0 < \tau < \infty$. Comparing Equation 5 with Equation 6 suggests that

$$\bar{\varepsilon}(u) = \sum_{n=1}^{m} (\varepsilon_{sn} - \varepsilon_{\infty n}) f(u) \quad (7)$$

and

$$\bar{\sigma}(u) = \varepsilon_o \bar{\varepsilon}(u)/\tau$$

or

$$\bar{\sigma}(u) = \frac{\varepsilon_o}{\tau_{oI}} \sum_{n=1}^{m} (\varepsilon_{sn} - \varepsilon_{\infty n}) \exp(-u) f(u) \quad (8)$$

However, enlarged use of network representation favours a discrete network rather than a distributed one. Consequently, the effective range of the variable u, estimated from either, $f(u)$ or $\bar{\varepsilon}(u)$, is represented by a parallel combination of L branches, each comprising a series connected resistive–capacitive elements, see Fig. 2. A branch element can simply be evaluated using Equations 7 and 8 provided that Δu is given. However, Δu is determined empirically during test. In the absence of an optimization rule in the approximation from the distributed to the discrete network, Δu can be considered as constant throughout the effective u range. Branch elements are then given by

$$\varepsilon_k \cong \varepsilon(u_k) \Delta u$$

and

$$\sigma_k \cong \frac{\varepsilon_k}{\tau_k}$$

where k designates a branch of u_k which is taken at the middle of Δu,

$$u_k = u_m + \left(k - \frac{1}{2}\right) \Delta u, \quad (9)$$

where u_m is the minimum u in the effective range.

The total parallel permittivity then becomes,

$$\varepsilon_t(\omega) = \varepsilon_\infty + \sum_{k=1}^{L} \frac{\varepsilon_k}{(1 + \omega^2 \tau_k^2)} \quad (10)$$

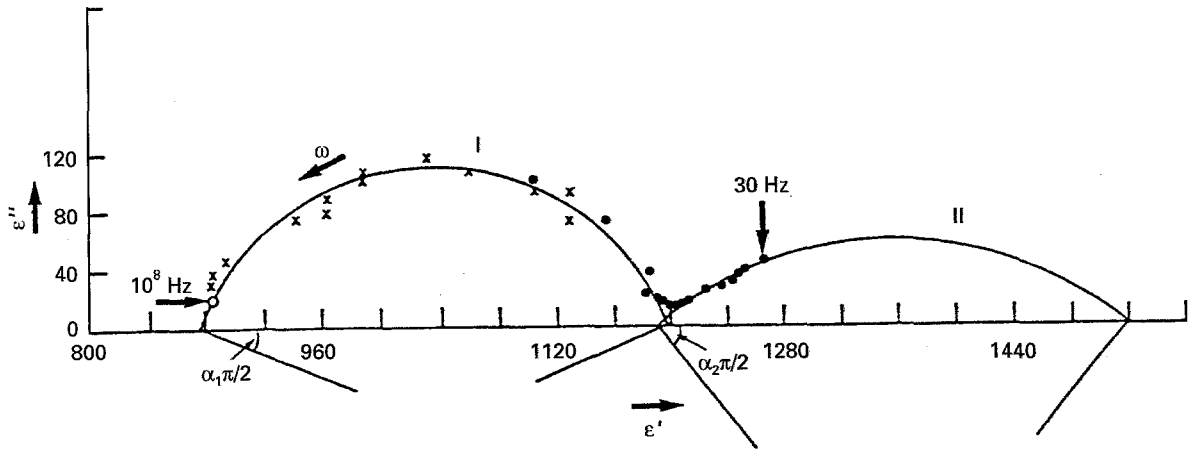

Figure 3 Cole–Cole plot for ZnO varistor. $T = 22\,^{\circ}C$. Arc I is reproduced from [13]. Arc II is reproduced from [14].

while the total parallel conductivity is given by Equation 2.

Using the procedure outlined above, an equivalent network is derived for zinc oxide varistors at low electric fields. Similarly, an equivalent network is also derived for perfluoropolyether microemulsion polymer. The validity of the network is then examined by comparison with experimental data.

3. Results and discussion

3.1. Zinc oxide varistor at low fields

Reported low-electric field data for ZnO varistors originating from different methods of measurement are shown in Fig. 3 [13]. A detailed account of data analysis in terms of the multiple-arc method is reported elsewhere [14]. The double arcs generated are characterized by the following parameters [14]:

$$\varepsilon_{sI} = 1195.0, \varepsilon_{\infty I} = 875.0, \tau_{oI} = 6.78 \times 10^{-7}\ \text{s}, \alpha_I = 0.233,$$

$$\varepsilon_{sII} = 1507.0, \varepsilon_{\infty II} = 1185.0, \tau_{oII} = 65.78 \times 10^{-3}\ \text{s},$$

$$\alpha_{II} = 0.555.$$

These parameters are then used to determine the network parameters $\bar{\sigma}(u)$ and $\bar{\varepsilon}(u)$ using Equations 7 and 8. $\bar{\sigma}(u)$ and $\bar{\varepsilon}(u)$ are displayed in Figs 4 and 5 where the u range from -16 to $+16$ corresponds to τ from 7.39×10^{-9} s to 5.83×10^{5} s, respectively.

The validity of the discrete network in representing dielectric dispersion is examined by comparing the measured dielectric constant with that obtained from the network model. This was achieved using Equations 7, 8 and 10. The interval Δu is taken as 1 over the effective range from -16 to 0, corresponding to approximately 22 MHz and 2.5 Hz, respectively. Subsequently, each interval is represented by the branch elements ε_k and ρ_k with τ_k evaluated by Equation 9. The network parameters of 16 branches are given in Table I. Comparisons are also made with the dispersion of a distributed network whereby Δu is approximated to 0.1. Over the frequency range of 30 Hz to 10 MHz, remarkable agreement was obtained when comparing measured dielectric constant with those computed from the distributed and discrete networks, as depicted in Fig. 6. Satisfactory agreement was also

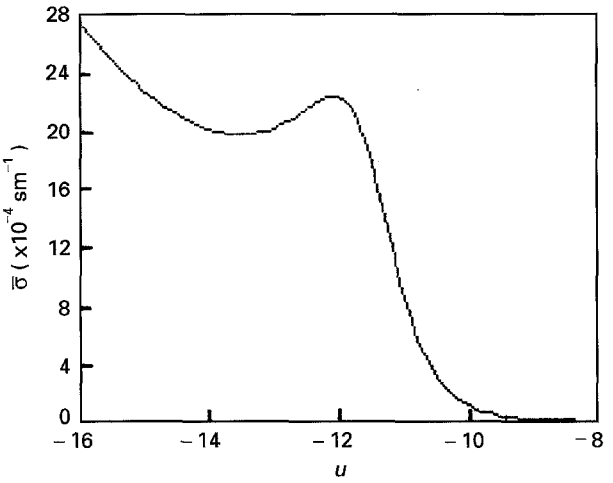

Figure 4 The distribution parameter $\bar{\sigma}(u)$ as a function of u for ZnO varistor.

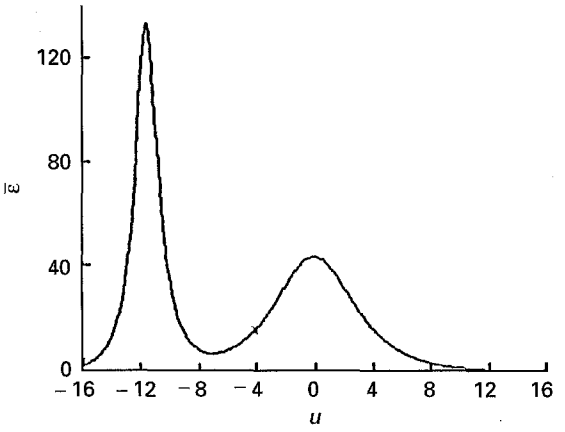

Figure 5 The distribution parameter $\bar{\varepsilon}(u)$ as a function of u for ZnO varistor.

found between measured and computed a.c. resistivities, as shown in Fig. 7. The same degree of agreement is also obtained for the dissipation factor, $\tan\delta$, as indicated by Fig. 8. The deviations from measured resistivity for frequencies greater than 1 MHz is likely to be attributed to the averaging nature of the arc-analysis, as indicated by arc (I) in Fig. 3. These deviations may partly be accounted for, in the high

TABLE I 16-branch network parameters for ZnO varistor

Branch no.	τ(s)	ε	ρ(Ωm)
1	1.22×10^{-8}	3.66	3.77×10^{2}
2	3.30×10^{-8}	8.24	4.53×10^{2}
3	9.00×10^{-9}	21.12	48.15
4	2.45×10^{-7}	62.34	444.1
5	6.65×10^{-7}	122.34	614.2
6	1.8×10^{-6}	65.5	3122.4
7	4.91×10^{-6}	23.18	2.394×10^{4}
8	1.34×10^{-5}	10.655	1.421×10^{5}
9	3.63×10^{-5}	7.12	5.761×10^{5}
10	9.78×10^{-5}	7.11	1.55×10^{6}
11	2.68×10^{-4}	9.14	3.31×10^{6}
12	7.29×10^{-4}	13.22	6.23×10^{6}
13	1.98×10^{-3}	19.28	1.16×10^{7}
14	5.39×10^{-3}	27.3	2.23×10^{7}
15	1.46×10^{-2}	35.9	4.6×10^{7}
16	3.98×10^{-2}	41.9	10.7×10^{7}

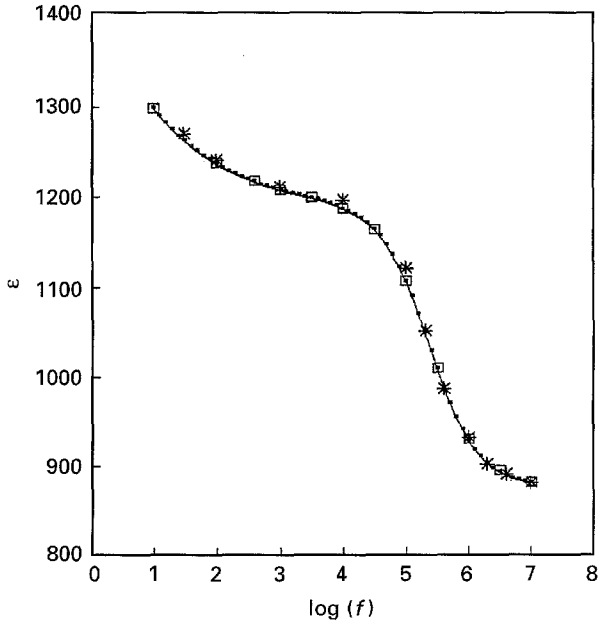

Figure 6 Comparison between computed and measured dielectric constant for ZnO varistor. —●— Computed from distributed network. □ Computed from discrete network. * Measured.

frequency range, by adding more network branches corresponding to a u-range below -16. It is anticipated that higher field analysis can be performed by measuring the dispersion of a small perturbing a.c. field superimposed on the high stressing d.c. field. The procedure outlined above can then be applied in the high stress region where a ZnO varistor becomes nonlinear dielectric.

3.2. Perfluoropolyether microemulsion

The procedure developed in section 2 has been applied to derive an equivalent circuit for a perfluoropolyether microemulsion dielectric. The reported components of complex dielectric constant were taken over the frequency range of 100 kHz to 100 MHz. Analysis of data yielded a single arc as depicted in Fig. 9. The arc is characterized by the following parameters;

$$\varepsilon_s = 202, \quad \varepsilon_\infty = 3, \quad \tau_o = 40\times10^{-9}\ \text{s}, \quad \alpha = 0.41$$

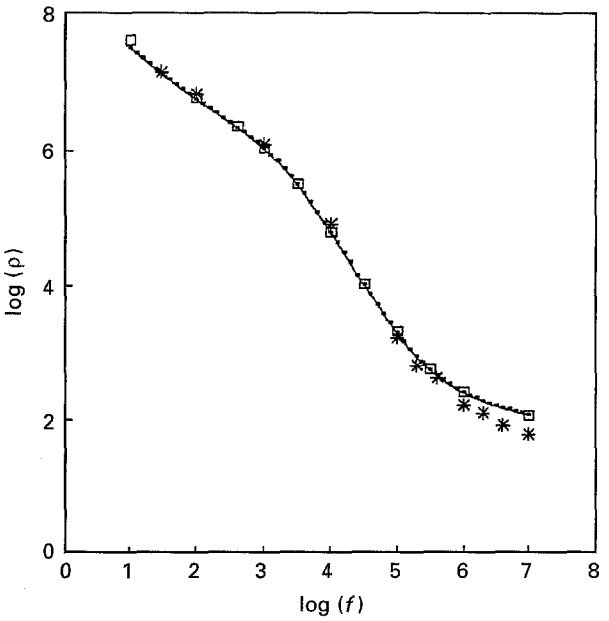

Figure 7 Comparison between computed and measured a.c. resistivites for ZnO varistor. —●— Computed from distributed network. □ Computed from discrete network. * Measured.

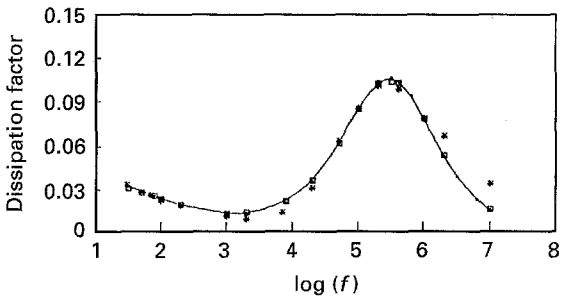

Figure 8 Comparison between computed and measured dissipation factor, tan δ, for ZnO varistor. —●— Computed from distributed network. □ Computed from discrete network. * Measured.

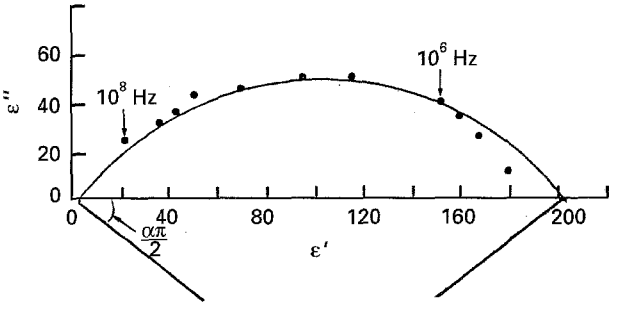

Figure 9 Cole–Cole plot for a perfluoropolyether microemulsion.

The corresponding $\bar{\sigma}(u)$ and $\bar{\varepsilon}(u)$ are shown in Figs 10 and 11, where the effective u-range from -10 to 10 corresponds to τ fom 1.82×10^{-12} to 8.81×10^{-4} s, respectively.

The procedure outlined in section 2 and applied to zinc oxide data has been used to derive the network branch parameters for a perfluoropolyether dielectric. Subsequently, with Δu taken as 1, and the effective u-range as 20, the discrete network parameters are determined and given in Table II, where 18 branches

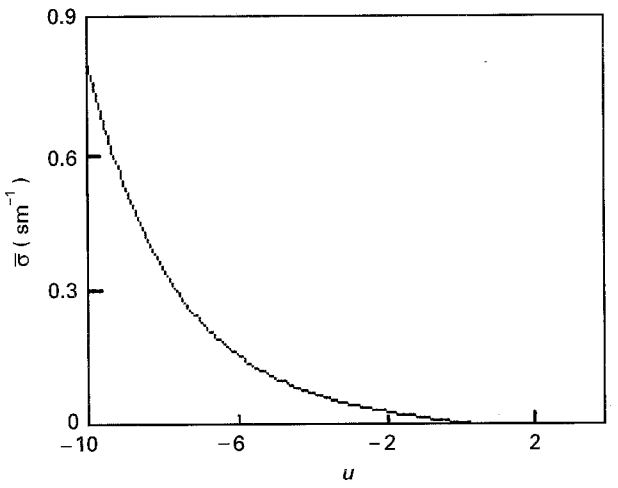

Figure 10 The distribution parameter $\bar{\sigma}(u)$ as a function of u for a perfluoropolyether microemulsion.

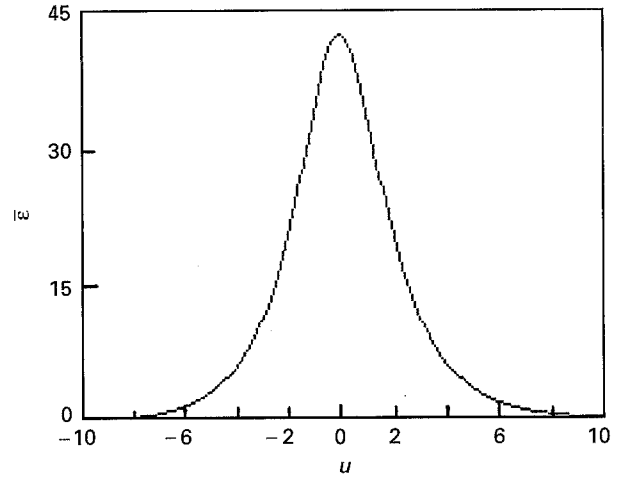

Figure 11 The distribution parameter $\bar{\varepsilon}(u)$ as a function of u for a perfluoropolyether microemulsion.

TABLE II 18-branch network parameters for a perfluoropolyether microemulsion

Branch no.	τ(s)	ε	ρ(Ωm)
1	3.07×10^{-12}	0.2276	1.524
2	8.34×10^{-12}	0.411	2.293
3	22.68×10^{-12}	0.7443	3.443
4	61.64×10^{-12}	1.350	5.159
5	167.6×10^{-12}	2.460	7.698
6	455.5×10^{-12}	4.5	11.438
7	1.24×10^{-9}	8.29	16.902
8	3.37×10^{-9}	15.26	24.954
9	9.15×10^{-9}	26.82	38.55
10	24.87×10^{-9}	39.15	71.78
11	67.6×10^{-9}	38.96	196.058
12	183.75×10^{-9}	26.82	744.15
13	499.5×10^{-9}	15.27	3696.2
14	1.36×10^{-6}	8.3	18.515×10^{3}
15	3.69×10^{-6}	4.5	92.655×10^{3}
16	10.03×10^{-6}	2.46	460.705×10^{3}
17	27.27×10^{-6}	1.35	22.82486×10^{5}
18	74.13×10^{-6}	0.745	112.43317×10^{5}

are indicated. The components of the remaining two branches were found to have negligible effects within the range of frequency used. A remarkable agreement was realized on comparing the measured and computed network parameters as indicated in Figs 12 and 13.

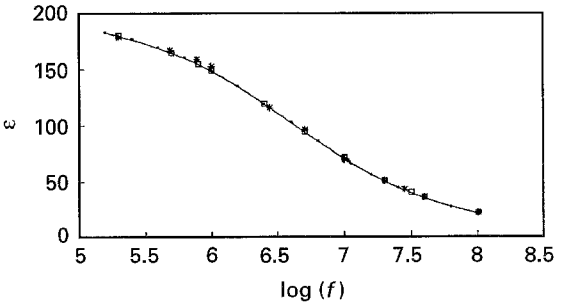

Figure 12 Comparison between computed and measured dielectric constant for a perfluoropolyether microemulsion. —●— Computed from distributed network. □ Computed from discrete network. * Measured.

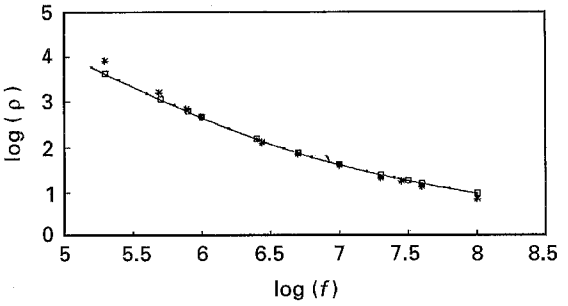

Figure 13 Comparison between computed and measured a.c. resistivities for a perfluoropolyether microemulsion. —●— Computed from distributed network. □ Computed from discrete network. * Measured.

4. Conclusions

The method of dielectric analysis presented in this paper has introduced two new parameters to characterize dispersion of the dielectric constant with frequency. The parameters are derived from multiple-arc analysis whereby circular arcs are described in the dielectric constant complex plane. The dispersion parameters have been shown to be effective in deriving a discrete network as demonstrated using the dispersion data of a ZnO varistor and a perfluoropolyether microemulsion. The close agreement between distributed and discrete networks makes the reduction of branch number feasible. Further work is underway to develop an optimizing rule to minimize the number of the network branches.

References

1. J. WOLAK, *IEEE Trans. E. I.* **28** (1993) 116.
2. M. GRAZIA GIRI, M. CARLA, C. M. C. GAMBI, D. SENATRA, A. CHITTOFRATI and A. SANGUINETI, *Meas. Sci. Technol.* **4** (1993) 627.
3. A. HADDAD, H. S. B. ELAYYAN, D. M. GERMAN and R. T. WATERS, *IEE Proc. A* **130** (1991) 265.
4. A. HADDAD, J. FUENTES-ROSADO, D. M. GERMAN and R. T. WATERS, *ibid.* **137** (1990) 269.
5. A. E. FLAK, B. M. LACQUET and P. L. SWART, *Electron. Lett.* **28** (1992) 166.
6. S. N. AL-REFAIE, *Appl. Phys.* **A51** (1990) 419.

7. *Idem, ibid.* **A52** (1991) 234.
8. S. N. AL-REFAIE and H. S. B. ELAYYAN, *J. Mater. Sci. Lett.* **12** (1993) 334.
9. H. S. B. ELAYYAN and S. N. AL-REFAIE, *J. Mater. Sci.: Mater. Electron.* **4** (1993) 74.
10. S. N. AL-REFAIE and H. S. B. ELAYYAN, *J. Mater. Sci.* **28** (1993) 2233.
11. V. V. DANIEL, "Dielectric Relaxation" (Academic Press, New York, 1976).
12. S. N. AL-REFAIE, *Appl. Phys.* **A55** (1992) 213.
13. L. M. LEVINSON and H. R. PHILIPP, *J. Appl. Phys.* **47** (1976) 1117.
14. S. N. AL-REFAIE and H. S. B. ELAYYAN, *J. Mater. Sci. Lett.* **11** (1992) 988.

Received 10 April
and accepted 17 July 1995